IEEE Access
Multidisciplinary | Rapid Review | Open Access Journal

Received 7 April 2025, accepted 24 May 2025, date of publication 2 June 2025, date of current version 10 June 2025.
Digital Object Identifier 10.1109/ACCESS.2025.3575908

RESEARCH ARTICLE

Application of Fuzzy Logic Sliding Mode Control Approach With PID Structure for Electro-Hydraulic Actuator Tracking System

MUHAMAD FADLI GHANI[1,2], (Member, IEEE), AHMAD ATHIF MOHD FAUDZI[1,2], (Senior Member, IEEE), ROZAIMI GHAZALI[3], (Senior Member, IEEE), AND SHAHROL MOHAMADDAN[4]
[1]Faculty of Electrical Engineering, Universiti Teknologi Malaysia, Skudai 81310, Malaysia
[2]Centre for Artificial Intelligence and Robotics, Universiti Teknologi Malaysia, Kuala Lumpur 54100, Malaysia
[3]Faculty of Electrical Technology and Engineering, Universiti Teknikal Malaysia Melaka, Durian Tunggal 76100, Malaysia
[4]College of Engineering, Shibaura Institute of Technology, Tokyo 135-8548, Japan

Corresponding author: Muhamad Fadli Ghani (m.fadli@utm.my)

This work was supported by the Research Management Center (RMC) at Universiti Teknologi Malaysia, through the Universiti Teknologi Malaysia Encouragement Research (UTMER) under Grant Q.J130000.3823.42J06.

ABSTRACT The electro-hydraulic actuator (EHA) system generates a trajectory by transferring high force densities in the form of pressurized fluid flows to a hydraulic actuator. Moreover, the sliding mode control (SMC) approach has been discovered as a potential method for the EHA trajectory tracking control system. However, high-frequency proportional valve activity has occurred during the practical application of the conventional SMC approach, resulting in tracking performance degradation. Furthermore, a preferable SMC sliding surface design is necessary to improve the precision of trajectory tracking performance, and the SMC designs involve complicated procedure and mathematical formulations. Therefore, this paper proposes a hybrid optimized fuzzy logic (FL) SMC with a proportional-integral-derivative (PID) structure (FLSMCPID) for trajectory tracking control in an EHA system. The proposed control strategy was designed with the switching function modification based on an FL approach in the conventional SMC algorithm. Due to the difficulty of concurrent hybrid design, a particle swarm optimization (PSO) algorithm was employed to determine the optimal control variables value. Simulations utilizing a linear EHA system model obtained using the grey-box identification approach and experimentation on an EHA system workbench for various trajectories and under the consequences of variation in supply pressure were conducted to evaluate the performance of the proposed control strategy. The simulation and experimental results demonstrate that higher effectiveness, precision, and robustness were achieved by the EHA system with the proposed control strategy.

INDEX TERMS High-frequency proportional valve, fuzzy logic sliding mode control with PID structure, Lyapunov theory, nonlinear system, nonlinear controller, particle swarm optimization.

I. INTRODUCTION

Electrohydraulic actuator (EHA) system evolved from the development of fluid power technology at the beginning of the 20^{th} century, which was first introduced by the French scientist Blaise Pascal in 1663. The informative overview of fluid power technology, which is also called hydraulic systems, was initially published by Merritt in 1967 and followed by Maskrey and Thayer in 1978 [1]. The first generation of hydraulic systems comprised of a flow control device driving an open loop hydraulic actuator. In line with the technology revolution, the EHA system is formed by the combination of the hydraulic system with electrical systems that control pressurized fluid flows from the motor pump to

The associate editor coordinating the review of this manuscript and approving it for publication was Wonhee Kim.

the electrohydraulic control valve by an electrical signal, and it will be transferred to the hydraulic actuator to generate a precise trajectory.

Modelling and control are the most critical procedures in the engineering design strategy for realizing advanced technology. In general, it is challenging to establish an accurate dynamic model when the EHA system is inherently uncertain, highly non-linear, and time-varying, which complicates modeling and controller design. Non-linear flow and pressure characteristics, backlash in control valves, actuator friction, fluctuations in trapped fluid volume caused by piston movement, and fluid compressibility all contribute significantly to the actuation system's non-linearity [2].

Even though the EHA system has several drawbacks, its current applications show how important hydraulic actuators are to modern technology. As can be observed from the literature, various articles have been published by academics and researchers about trajectory tracking control utilizing the EHA system due to its broad variety of applications [3], [4], [5], [6], [7], [8], [9], [10], [11]. Therefore, the emphasis of this research will be on various types of EHA system control strategies, specifically for trajectory tracking control.

Recently, the EHA systems have been broadly utilized in industrial hydraulics such as hydraulic presses [12], work-holding systems [13], injection molding machines [14], electrohydraulic excavators [15], and drill rigs [16] due to their high power, force, and linear mobility. Meanwhile, according to Industry 4.0, which was established by the German government in 2013 [17], [18], the industrial hydraulic systems were set up with higher standards to produce intelligent EHA systems. As a result of advancements in manufacturing technology, electronic equipment, and computers, the development of EHA control systems is critical to meeting new needs, particularly in terms of high-frequency response, which has become the motivation for this study.

Intensive studies have been observed relating to the EHA for a wide variety of applications in current industrial tracking systems, for instance in robotics [19], [20], motion simulators [21], [22], [23], [24], fatigue testing systems [25], and mining [26], [27]. Nowadays, with the rapid development in computer technology and control theory, the process of modeling the non-linear dynamic behavior of the EHA systems can be expected to be implemented in excellent circumstances and produce highly precise models. Consequently, conventional feedback controls, such as proportional-integral-derivative (PID) controllers, that have the advantage of being easy to tune, can be replaced with advanced model-based control methods such as the sliding mode control (SMC) approach, so that high performance tracking control can be formed, which has also become a motivation for this study.

The SMC is a variable-structure controller whose primary design is based on the Lyapunov stability theory, assuring the overall stability of the EHA system's bounded input and bounded output [28], [29]. However, the undesired characteristic of oscillations with finite frequency and amplitude has emerged in practical applications of the SMC associated with EHA systems, which cause damage to the system's final control element and degrade the tracking control performance [30]. As a result, improvement approaches such as modifications to the sliding surface design, reaching law methods, higher order designs, and hybrid designs can be explored and developed to improve the conventional SMC controller performance in terms of tracking and disturbance rejection capabilities which turned out to be another motivation for this study.

The trajectory tracking control using the SMC approach has been discovered as a very potential method for the EHA control systems due to its significant robustness to uncertainties and disturbances. However, high-frequency proportional valve activity which is in the maximum range of 50 to 150 Hz has occurred in practical applications of the conventional SMC approach in the EHA system, resulting in performance degradation of the trajectory tracking control [31], [32]. Numerous studies have been undertaken to improve the trajectory tracking control performance, and it was determined that the discontinuous signum function in the conventional SMC algorithm was the cause of the issue. To overcome this issue, a well-designed continuous switching function in the SMC algorithm has to be developed. In addition, a preferable structure design of the sliding surface in the SMC algorithm can effectively improve the precision of trajectory tracking performance in the EHA system. Thus, it is necessary to design a hybrid sliding surface with linear control in the SMC algorithm that consequently will improve the precision of trajectory tracking with significant robustness in the EHA system under variation of supply pressure. Besides, the SMC designs are involved with complicated rules and mathematical formulations due to their strong reliance on analytical approaches [33]. Therefore, numerous researchers find it difficult to implement analytical approaches for the SMC controller design into practice. In certain circumstances, the analytical approaches must be revised for each change in the EHA system's dynamic behavior, particularly when supply pressure varies, which is inefficient in practical implementations. Recently, Han, showed that the metaheuristic approach is efficient for optimizing the control variables of SMC design [34].

Various combinations of fuzzy logic, SMC, and PID techniques have been investigated in recent works on tracking control of EHA system in order to manage the system's inherent nonlinearities, parameter fluctuations, and external disturbances. Although they are straightforward and provide dependable steady-state performance, conventional PID controllers frequently have trouble with nonlinear behaviors and abrupt load changes in EHA system. Because of its durability and strong rejection of disturbances, SMC has been used; nonetheless, it has high-frequency valve activity issue and may need precise system modeling. Although fuzzy logic controllers (FLCs) are more flexible and can handle system uncertainties without exact modeling, they are not as good at tracking in steady-state scenarios [35]. Current hybrid techniques, including fuzzy-PID and fuzzy-SMC, try to capitalize on each technique's advantages [36]. However, because of the difficulties in rule-based optimization and computing complexity, these approaches frequently have limitations in terms of real-time performance. The practical applicability of many existing studies is limited due to their lack of thorough validation on physical EHA systems, despite their promising nature. Creating real-time implementable, low-complexity hybrid controllers that can provide high precision, resilience, and flexibility in dynamic EHA situations is still a key gap. Therefore, it is crucial to design an effective, precise, and robust control strategy in the EHA system based on the SMC approach for trajectory tracking control by employing a well-established metaheuristic approach with fewer complex mathematical formulations. The main contributions of this work are itemized below.

- This paper investigates the modified fuzzy logic sliding mode control (FLSMC) designed based on the switching function modification in the conventional SMC algorithm using the FL approach.
- This paper also contributes to the design of a hybrid sliding surface in the FLSMC algorithm with PID control called FLSMCPID, to improve the precision of tracking control performance for various trajectories with considerable robustness. The variables for the FLSMCPID control strategy are optimized using the PSO procedure. Simulation and experimental results demonstrate that the proposed FLSMCPID control strategy in the EHA system can achieve great precision improvement in trajectory tracking control performance with significant robustness.

The rest of the paper is organized in the following manner. Experimental design is briefly introduced and defined in Section II. The EHA system model is described in Section III. The control strategy designs are defined in Section IV. Simulation and experimental results are presented and analyzed in Section V. Finally, conclusions and future works are given in Section VI.

II. EXPERIMENTAL DESIGN

An EHA system workbench with an instrumented experimental system, as shown in Fig. 1, was designed for experimental measurements of assessment and verification. The EHA system workbench consists of a real-time control system based on MATLAB and PCIe-6321, a moving cylinder, and a hydraulic power supply with an 8 MPa supply pressure and 16.6 L/min flow capacity. The hydraulic cylinder has a 40 mm bore and a 25 mm rod. It is controlled by a proportional directional valve with a maximum flow rate of 80 L/min and a maximum supply pressure of 31.5 MPa. A wire displacement sensor is used to measure the cylinder's displacement in real time.

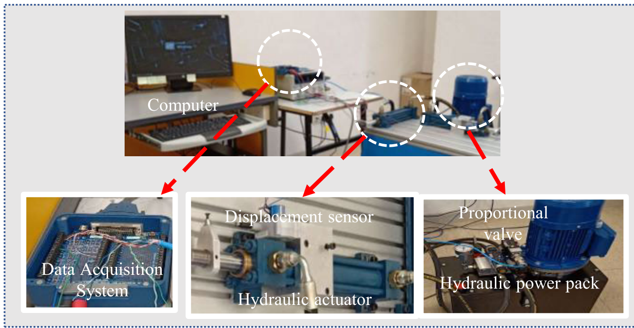

FIGURE 1. The EHA system experimental design.

In general, while building an EHA system workbench, the proportional directional valve is positioned sufficiently near to the double-acting hydraulic actuator so that the pipeline dynamics may be neglected. Input-output behavior is unaffected by pipeline effects during low-frequency operation. Consequently, the power supply unit is designed such that the systems maintain a consistent power supply pressure across a certain operating range. In addition, a well-designed proportional directional valve was used to eliminate non-linearities and uncertainties in dynamic performance. Due to the faster speed of dynamic reaction of the proportional directional valve compared to the dynamic response of the actuator, the dynamics of the proportional directional valve are always neglected.

The control system for the EHA system is shown in physical detail in Fig. 2. It represents the hardware and software configuration for data collection for this research. The control hardware consists of a host computer, a PCIe-6321 16-bit A/D and D/C card for receiving sensor signals and transmitting control signals, as well as various additional devices.

The host computer serves as an operator interface for human-computer interaction and integrates with the PCIe-6321 card. The proposed control algorithm is programmed and executed on the host computer using MATLAB/Simulink, together with the comparative approaches. In order to assure acceptable performance, 1 kHz has been selected as the sample rate for the experimental system. During the experiment execution, the computer's digital output was sent to the DAQ system, which generated a voltage signal and delivered it to the proportional directional valve. The proportional directional valve then controls the flow of pressurized fluid to the double-acting hydraulic actuator, resulting in a controlled piston displacement. The wire displacement sensor measured the piston's trajectory. Finally, the sensor signal was transformed into a digital signal by the DAQ system and transmitted back to the computer unit. The collected data from the experiments was analyzed and compared to the simulation data analysis in time domain, where the response patterns were observed and compared, to validate the results. The closed-loop experiments were also carried out at various supply pressures to assess the proposed controller's performance and robustness.

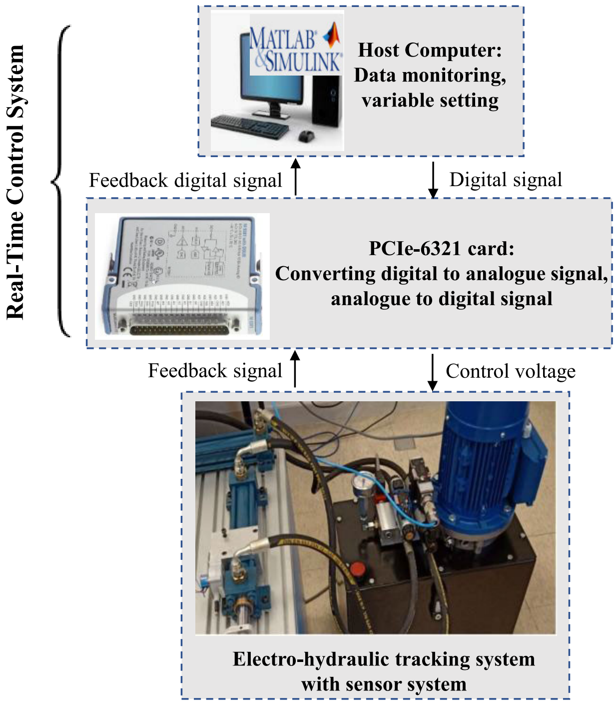

FIGURE 2. Control schematic diagram for EHA system workbench.

III. EHA SYSTEM MODEL

The EHA system's model linearization has been used for decades to deal with the non-linearities that exist in the modeling process. Numerous researchers have successfully employed linear models in their proposed control strategies [37], [38], [39], [40], [41], [42], [43]. In practice, most physical systems will have unpredictable dynamic behavior and non-linearities. Therefore, the mathematical model may likewise be expressed in a non-linear structure. For further exploration, it is necessary to represent both the physical system and the mathematical model as a linear model, which can represent the essential dynamic characteristics at least within one operational point. It is well-known that a linear model is sufficient for tracking control with advanced control strategies to achieve high performance of an EHA system in trajectory tracking applications, and Merritt [1] also concludes that the linear model of an EHA system is often valid across a relatively broad range.

In this research, a parametric method was utilized since it emphasizes more on the mathematical aspect of obtaining a practical linear model of the EHA system. Furthermore, when utilizing a non-parametric method, the findings are simple to acquire, but the resultant model may be inaccurate at times. The parametric grey-box approach is used for identifying the linear EHA system model by considering prior knowledge of the system, which produces more accurate parameter estimations. This approach is associated with the physical modeling of the double-acting EHA system based on first principle of physical laws and parameter estimation processes [44], [45].

In this section, physically based modeling of the EHA system is performed to provide prior knowledge on mathematical model structure with regard to related dynamics and non-linearities. The mathematical model is derived from fundamental physical laws such as the laws of Newton and equilibrium equations. In addition, contributions from the literature on the theoretical modeling of hydraulic systems are used and considered. As described in [46], a mathematical model of the EHA system in Fig. 3 can be derived by ignoring non-linearities such as internal or external leakage and the dynamics of the valve. The system consists of a 4/3-way proportional valve, a double-acting cylinder, and a variable load force. The load involves of a mass that is adjustable. The supply pressure (P) is assumed to be constant, and the control purpose is the trajectory of the payload. In addition, Q_A and Q_B are the net flow rates through the control ports A and B, respectively. The mathematical model is derived from the proportional valve's flow rate equation, the continuity equation, and the balance of forces at the cylinder piston. The valve flow rate equation is extremely non-linear and is proportional to the input voltage (u) and the pressure drop (P_L) across the load. As a result, the dynamics of the double-acting EHA system for total oil flow rates (Q_L) are obtained from a Taylor series linearization depicted by (1), where K_q and K_c are flow-gain coefficient and flow-pressure coefficient, respectively.

$$Q_L = K_q u - K_c P_L \tag{1}$$

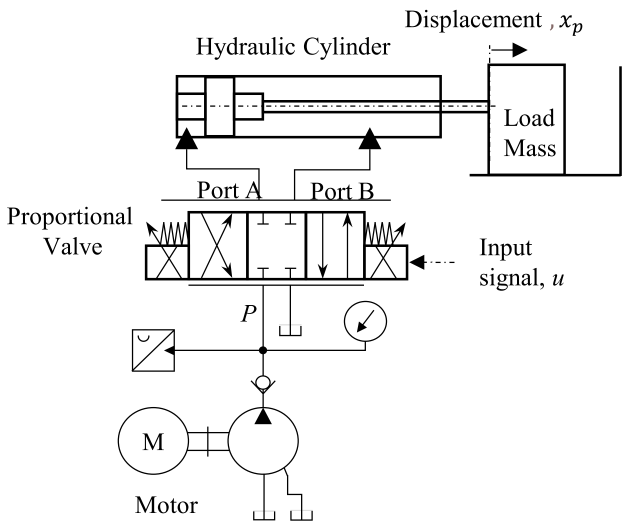

FIGURE 3. Schematic diagram of the double-acting EHA system.

Further factors that affect the Q_L include changes in oil volume owing to compressibility as well as cylinder movement and leakage oil flow as given by

$$Q_L = A_p \dot{x}_p + \frac{V_t}{4\beta_e}\dot{P}_L + f(P_L) \tag{2}$$

where V_t, A_p, $\dot{x}_p$, β_e, and $f(P_L)$ are the total compressed oil volume, cylinder piston surface area, cylinder piston velocity, effective bulk-modulus coefficient, and function of internal and external oil leakage non-linear influence, respectively. It is assumed that the piston's rod and head are of equal size in this situation. If the leakage function $f(P_L)$ is approximated by a linear relation, (2) can be written as (3), where C_{tp} is the total leakage coefficient of the cylinder piston.

$$\dot{P}_L = \frac{4\beta_e}{V_t}(Q_L - A_p\dot{x}_p - C_{tp}P_L) \tag{3}$$

In the absence of non-linear effects of dry and adhesive friction, the force F_a generated by the cylinder piston and directed to the load mass M_t positioned on the piston's end is determined by

$$F_a = A_P P_L = M_t\ddot{x}_p \tag{4}$$

Finally, the mathematical model structure based on the transfer function depicted by (6) is obtained by combining (1), (3), and (4) and applying the Laplace transformation to the resultant third-order differential equation in (5).

$$\begin{aligned}\frac{M_t\dddot{x}_p}{A_P} &= \frac{4\beta_e}{V_t}(K_q u - (K_c + C_{tp})\frac{M_t\ddot{x}_p}{A_P} - A_p\dot{x}_p)\dddot{x}_p \\ &= \frac{4A_P\beta_e}{M_tV_t}K_q u - \frac{4\beta_e}{V_t}\left(K_c + C_{tp}\right)\ddot{x}_p - A_P^2\frac{4\beta_e}{M_tV_t}\dot{x}_p \\ &= a_2 u - a_1\ddot{x}_p - a_0\dot{x}_p \end{aligned} \tag{5}$$

$$\begin{aligned} s^3X_p(s) = a_2U(s) - a_1s^2X_p(s) - a_0sX_p(s)\ \frac{X_p(s)}{U(s)} \\ = \frac{a_2}{s\left(s^2 + a_1s + a_0\right)} \end{aligned} \tag{6}$$

where the abbreviations are as follows

$$a_0 = \frac{4A_p^2\beta_e}{M_tV_t} \tag{7}$$

$$a_1 = \frac{4\beta_e}{V_t}\left(K_c + C_{tp}\right) \tag{8}$$

$$a_2 = \frac{4A_P\beta_e}{M_tV_t}K_q \tag{9}$$

Furthermore, the parameter estimation of the mathematical model in (6) is obtained using the MATLAB System Identification toolbox. The EHA system workbench with configuration shown in Fig. 2 was used to collect data for the open-loop experiment and the sum of sinusoidal signals was employed as an input signal for this process. This form of signal was also used in [47] during the identification procedure, specifically for the EHA system. The general representation for the sum of sinusoidal signals can be seen in (10), where b_i is the signal amplitude, and f_i is the input frequency. The value p is determined by the number of the model parameters.

$$u(t) = \sum_{i=1}^{p} b_i \sin(2\pi f_i t) \tag{10}$$

It can be seen in (6) that there are three model parameters that need to be estimated. Therefore, the input signal in (11) was developed and used for the open-loop experiment, which was generated at three different frequencies and amplitudes.

$$u(t) = 0.5\sin(2\pi 0.05t) + 1.5\sin(2\pi 0.2t) + 2\sin(2\pi t) \tag{11}$$

Then, the collected data was loaded into the MATLAB System Identification toolbox and trend filtering was performed. The model structure based on (6) was then chosen, and finally, model fitting was performed for parameter estimates and validation.

IV. CONTROL STRATEGY DESIGN

This section describes and formulates in detail the design algorithm of the FLSMC and FLSMCPID control strategies. This includes the process of obtaining optimal control variables using a PSO algorithm and the Lyapunov theorem for theoretical stability analysis of the designed control strategies. Furthermore, the SMC and hybrid SMC with PID (SMCPID) approach are briefly explained as benchmarking control schemes to further verify the effectiveness, precision, and robustness of the proposed control strategies.

A. SMC AND FLSMC DESIGNS

The block diagram of the closed-loop EHA system can be seen in Fig. 4, where r and x_p are the reference trajectory and piston trajectory signals, respectively. Meanwhile, e is the system tracking error, which is defined as

$$e = r - x_p \tag{12}$$

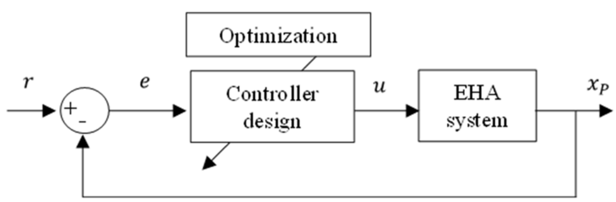

FIGURE 4. The closed-loop block diagram of an EHA system.

The most important step in the SMC and FLSMC designs is known to be coming up with the mathematical equation for the sliding surface. Therefore, (13) was considered in this research to represent the sliding surface, s for the SMC and FLSMC design, where λ is the control gain coefficient factor of the sliding surface and n is the order for the model of the EHA system [48].

$$s = \left(\lambda + \frac{d}{dt}\right)^{n-1} e; \lambda > 0, n > 1 \tag{13}$$

The linear EHA system model was developed as a third-order mathematical model structure in (6). Hence, (13) can be revised as

$$\begin{aligned} s &= \left(\lambda + \frac{d}{dt}\right)^2 e \\ &= \lambda^2 e + 2\lambda\dot{e} + \ddot{e} \end{aligned} \tag{14}$$

Furthermore, the differentiation of (14) and incorporating with (5) and (12) can be represented as in (15). Additionally, a reaching law is required to compel the EHA system output x_p to follow the design sliding surface (14) and keep the EHA closed-loop system in stable condition. The reaching law-based for sliding mode involves a reaching phase and a sliding phase. During the reaching phase, the system is bound to reach the sliding surface in a finite amount of time from any initial state, whereas during the sliding phase, the system is constrained to slide on the sliding surface.

$$\begin{aligned}\dot{s} &= \lambda^2\dot{e} + 2\lambda\ddot{e} + \dddot{e} \\ &= \lambda^2\dot{e} + 2\lambda\ddot{e} + (\dddot{r} - \dddot{x}_p) \\ &= \lambda^2\dot{e} + 2\lambda\ddot{e} + \dddot{r} - a_2 u + a_1\ddot{x}_p + a_0\dot{x}_p \qquad (15)\end{aligned}$$

According to [28], there are four established reaching laws which are constant rate, exponential, power rate, and general reaching laws. However, the exponential reaching law, as represented in (16), where ε and k are constants and *sign(s)* is the signum function, was employed in this research. This law was utilized as it consists of proportional rate term *-ks*, which can compel the state of the EHA system to approach the sliding phase more quickly when s is large.

$$\dot{s} = -\varepsilon sign(s) - ks;\ sign(s) = \begin{cases} 1 & for\ s > 0 \\ 0 & for\ s = 0 \\ -1 & for\ s < 0 \end{cases} \qquad (16)$$

By solving for (15) and (16), the control algorithm for the SMC approach was established and can be expressed as

$$u_{SMC} = \frac{\lambda^2\dot{e} + 2\lambda\ddot{e} + \dddot{r} + a_1\ddot{x}_p + a_0\dot{x}_p}{a_2} + \frac{\varepsilon sign(s) + ks}{a_2} \qquad (17)$$

However, the SMC causes high-frequency proportional valve activity due to discontinuity in the signum function that occurs throughout the control operation. To address this issue, this research utilized a continuous FL-based function to replace the signum function in the control algorithm of the SMC approach. The MATLAB Fuzzy Logic toolbox was used to establish the continuous FL function with a single-input and single-output structure, where the sliding surface range was estimated between -1×10^7 and 1×10^7, which used as the input. As shown in Fig. 5, three triangular input membership functions (MFs) were used, which are denoted as fuzzy logic negative input (FLNI), fuzzy logic zero input (FLZI), and fuzzy logic positive input (FLPI). Meanwhile, as indicated in Fig. 6, three output MFs: fuzzy logic negative output (FLNO), fuzzy logic zero output (FLZO), and fuzzy logic positive output (FLPO) were used to represent the output structure of the continuous FL function.

Furthermore, the Mamdani type min-max inference and the center of gravity defuzzification approach were applied

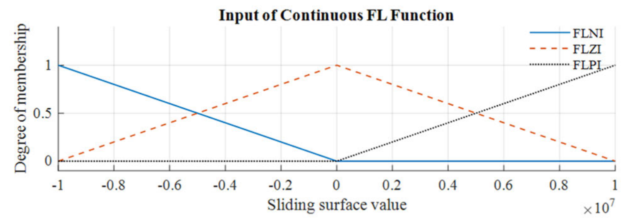

FIGURE 5. Input membership functions.

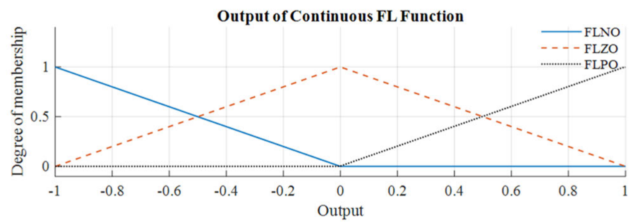

FIGURE 6. Output membership functions.

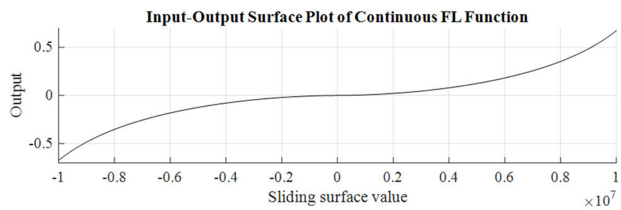

FIGURE 7. Input-output surface plot.

in this research. The consequent action of the input output profile is shown in Fig. 7, implying a rule-based design.

In this research, the developed FL function is denoted as *fuzz()*. Therefore, the exponential reaching law in (16) can be modified as in (18), where the output range of *fuzz(s)* is between -0.67 and 0.67 as can be seen in Fig. 9.

$$\dot{s} = -\varepsilon fuzz(s) - ks \qquad (18)$$

By solving for (15) and (18), the control algorithm of the FLSMC control strategies was established and can be expressed as

$$u_{FLSMC} = \frac{\lambda^2\dot{e} + 2\lambda\ddot{e} + r + a_1\ddot{x}_p + a_0\dot{x}_p}{a_2} + \frac{\varepsilon fuzz(s) + ks}{a_2} \qquad (19)$$

B. SMCPID AND FLSMCPID DESIGNS

The sliding surface in the FLSMC algorithm written in (14) was altered to a hybrid sliding surface with PID control, which resulted in the FLSMCPID algorithm. For both FLSMCPID and SMCPID control strategies, the sliding surface is based on the modification in (14) to a hybrid sliding surface with PID control, which is written as

$$s = \left(k_p + k_i\int dt + k_d\frac{d}{dt}\right)^n e \qquad (20)$$

where k_p, k_i, and k_d are constant and n is the order for the model of the EHA system.

The linear EHA system model was developed as a third-order mathematical model structure in (6). Hence, (20) can be revised as

$$s = \left(k_p + k_i \int dt + k_d \frac{d}{dt}\right)^2 e$$
$$= k_p^2 e + 2k_p k_i \int edt + 2k_p k_d \dot{e} + 2k_d k_i e + k_i^2 \left(\int edt\right)^2 + k_d^2 \ddot{e} \quad (21)$$

Furthermore, the differentiation of (21) and incorporating with (5) and (12) can be represented as in (22).

$$\dot{s} = k_p^2 \dot{e} + 2k_p k_i e + 2k_p k_d \ddot{e} + 2k_d k_i \dot{e} + k_i^2 e \int edt + k_d^2 \dddot{e}$$
$$= k_p^2 \dot{e} + 2k_p k_i e + 2k_p k_d \ddot{e} + 2k_d k_i \dot{e} + k_i^2 e \int edt + k_d^2 (\dddot{r} - \dddot{x}_p)$$
$$= k_p^2 \dot{e} + 2k_p k_i e + 2k_p k_d \ddot{e} + 2k_d k_i \dot{e} + k_i^2 e \int edt + k_d^2 (\dddot{r} - a_2 u + a_1 \ddot{x}_p + a_0 \dot{x}_p) \quad (22)$$

By solving for (22) and (16), the control algorithm of the SMCPID approach was established and can be expressed as

$$u_{SMCPID} = \frac{k_p^2 \dot{e} + 2k_p k_i e + k_i^2 e \int edt}{a_2 k_d^2} \; \& \; + \frac{\varepsilon sgn(s) + ks}{a_2 k_d^2} + \frac{2k_p \ddot{e} + 2k_i \dot{e}}{a_2 k_d} + \frac{r + a_1 \ddot{x}_p + a_0 \dot{x}_p}{a_2} \quad (23)$$

Besides, by solving for (22) and (18), the control algorithm of the FLSMCPID control strategy was established and can be expressed as

$$u_{FLSMCPID} = \frac{k_p^2 \dot{e} + 2k_p k_i e + k_i^2 e \int edt}{a_2 k_d^2} + \frac{\varepsilon fuzz(s) + ks}{a_2 k_d^2} + \frac{2k_p \ddot{e} + 2k_i \dot{e}}{a_2 k_d} + \frac{r + a_1 \ddot{x}_p + a_0 \dot{x}_p}{a_2} \quad (24)$$

C. LYAPUNOV THEOREM: STABILITY ANALYSIS

The primary objective of the controller design is to guarantee that the feedback control of EHA system operates continuously in a steady manner. Consequently, the Lyapunov theorem approach can be applied to confirm the stability of the designed controllers. In dynamic system and control theory, this theorem is often used for stability analysis. The Lyapunov function with the constraint of $V(0) = 0$ and $V(t) > 0$ for $s \neq 0$ written as in (25) is used in this research. According to the Lyapunov stability theorem, the controller stability is ensured by a reaching condition expressed in (26). The reaching condition occurred when the trajectories from the reaching phase can reach the sliding phase which can be seen in Fig. 6.

$$V = \frac{1}{2} s^2 \quad (25)$$
$$\dot{V} = s\dot{s} < 0, \quad s \neq 0 \quad (26)$$

Therefore, to guarantee controller stability with smooth trajectory transitions from the reaching to the sliding phase, the exponential reaching law in (16) that was used for the SMC and SMCPID controller designs and the new modified exponential reaching law in (18) that was used for the FLSMC and FLSMCPID controller designs must adhere to the reaching condition.

By substituting the exponential reaching law in (16) into (26) produces

$$\dot{V} = -s(\varepsilon sign(s) + ks) \quad (27)$$

While $s > 0$, $sign(s) = 1$, and (27) yields

$$\dot{V} = -|s|(|\varepsilon|(1) + |k||s|)$$
$$= -|s|(|\varepsilon| + |k||s|) < 0 \quad (28)$$

While $s < 0$, $sign(s) = -1$, and (27) yields

$$\dot{V} = -s(|\varepsilon|(-1) + |k| s)$$
$$= -s(-|\varepsilon| + |k| s) \quad (29)$$

By assume that $s = -|\Delta|$ to represent the condition of $s < 0$, (29) can be expressed as

$$\dot{V} = -(-|\Delta|)(-|\varepsilon| + |k|(-|\Delta|))$$
$$= -|\Delta|(|\varepsilon| + |k||\Delta|) < 0 \quad (30)$$

As revealed by (28) and (30), $\dot{V} < 0$, which state that the design of the SMC and SMCPID approaches for tracking control in the EHA system using the exponential reaching law in (16) will be stable for the entire trajectory tracking operation.

Furthermore, by substituting the modified exponential reaching law in (18) into (26) produces

$$\dot{V} = -s(\varepsilon fuzz(s) + ks) \quad (31)$$

While $s > 0$, the output of FL function is bounded by a range of positive real numbers. Hence, by assuming that $fuzz(s > 0) = |\nabla|$, (31) can be expressed as

$$\dot{V} = -|s|(|\varepsilon| fuzz(s) + |k||s|)$$
$$= -|s|(|\varepsilon||\nabla| + |k||s|) < 0 \quad (32)$$

While $s < 0$, the output of FL function is bounded by a range of real negative numbers. Therefore, by assuming that $fuzz\,(s < 0) = -|\nabla|$ and $s = -|\Delta|$, (31) can be expressed as

$$\begin{aligned}\dot{V} &= -s\,(|\varepsilon|\,fuzz\,(s) + |k|\,s) \\ &= -(-|\Delta|)\,(|\varepsilon|\,(-|\nabla|) + |k|\,(-|\Delta|)) \\ &= -|\Delta|\,(|\varepsilon|\,|\nabla| + |k|\,|\Delta|) < 0 \qquad (33)\end{aligned}$$

As revealed by (32) and (33), $\dot{V} < 0$, which state that the design of the FLSMC and FLSMCPID control strategies using the modified exponential reaching law in (18) will be stable for the entire trajectory tracking operation.

D. PSO ALGORITHM

The PSO algorithm was utilized to obtain optimum values for the SMC, FLSMC, SMCPID, and FLSMCPID controls design variables, and its algorithm was designed by mimicking the swarm social behavior of bird flocking and fish schooling. A swarm of individuals called particle i move through a high-dimensional search space among the entire population, ρ towards the global optimal solution with a specific position and velocity. Each particle i in the swarm offers a great solution and adheres to a simple principle by replicating its own previous success.

Furthermore, the personal best position, $pbest_{ij}$ in a neighborhood influences the position of particle i and the optimal solution among the personal best positions is known as the global best position, $gbest_{ij}$. The searching process starts with two initial particle parameters, namely position, X_{ij}^N and velocity, V_{ij}^N where N is the number of iterations. The new particle velocity, V_{ij}^{N+1} and particle position, X_{ij}^{N+1}, are adjusted and updated as

$$\begin{aligned}V_{ij}^{N+1} &= wV_{ij}^N + c_1 r_1 \left(pbest_{ij} - X_{ij}^N\right) \\ &\quad + c_2 r_2 (gbest_j - X_{ij}^N) \qquad (34)\end{aligned}$$

$$X_{ij}^{N+1} = X_{ij}^N + V_{ij}^{N+1} \qquad (35)$$

where w had been designed as in (36), for better particle exploration and exploitation, starting at 0.9 and decreasing linearly to 0.4 at the maximum iteration. Moreover, r_1 and r_2 represent random function values, while C_1 and C_2 are positive learning factors that control the strength of cognitive and social acceleration coefficients, respectively.

$$w = 0.9 - \frac{N}{\max N}(0.9 - 0.4) \qquad (36)$$

In addition, Fig. summarized the overall design process using the PSO algorithm. In this process, the particle's population size, maximum iteration, cognitive coefficient, and social coefficient were set as 20, 50, 2, and 2, respectively [49]. In relation to the SMC and FLSMC controllers' variables, as can be seen in (17) and (19), the position, X_{ij}^k was specified as

$$X_{ij}^N = \left[\lambda_{i1}^N \quad \varepsilon_{i2}^N \quad k_{i3}^N\right] \qquad (37)$$

Meanwhile, in relation to the SMCPID and FLSMCPID controllers' variables, as can be seen in (23) and (24), the position, X_{ij}^k was identified as

$$X_{ij}^N = [k_{p_{i1}}^N \quad k_{i_{i2}}^N \quad k_{d_{i3}}^N \varepsilon_{i4}^N \quad k_{i5}^N] \qquad (38)$$

Furthermore, a fitness function based on the sum of square error (SSE) represented in (39) was used to evaluate the performance of each individual particle where the particle was required to has a minimal fitness value.

$$J = \sum (r - x_p)^2 \qquad (39)$$

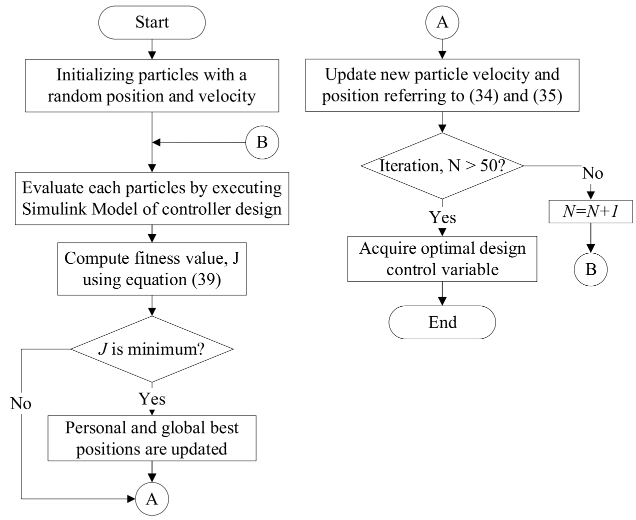

FIGURE 8. The overall design process using PSO algorithm.

E. TRAJECTORY TRACKING PROFILE

Several trajectories were developed to demonstrate the effectiveness of the proposed control strategies for tracking control in the EHA system. In both simulation and experimental exercises, four trajectories with their own unique signal design characteristics were developed. The sinusoidal, multi-sinusoidal, point-to-point, and chaotic trajectories will be employed to evaluate the proposed control strategies tracking control performance.

Sinusoidal trajectory, also known as the bandwidth test, is used to verify the highest frequency at which the control strategy can reliably track a specified trajectory's amplitude. However, the bandwidth test of the EHA system for tracking control is limited to 1 Hz due to hardware limitations. Thus, the performance of the investigated system may be evaluated to its limitations and capabilities under certain operating conditions. The sinusoidal trajectory generates a varying range of velocity and acceleration in the signal waveform, with the highest frictional effects occurring during the low-velocity condition and while reversing the actuator motion in the EHA system.

Meanwhile, the multi-sinusoidal trajectory was designed to generate a varying range of velocity and acceleration in the signal waveform with various specified amplitudes and operating frequencies. In addition, this trajectory is used to verify the proposed control strategies' tracking control performance to track a specified trajectory's amplitude within various operating frequency conditions. The multi-sinusoidal trajectory was developed with three different frequencies: 0.05 Hz, 0.1 Hz, and 0.2 Hz, which generated a varying range of velocity and acceleration in the signal waveform with several specified amplitudes and will be used to test the performance of the proposed control strategies in the EHA system. In addition, this trajectory also will be employed for validation of the dynamic model. In addition, the related sinusoidal-based trajectory tracking for the EHA system was used by many previous studies to examine the effectiveness of the designed control strategies [50], [51].

Furthermore, point-to-point tracking control is extensively used in robotic and industrial applications since it is the most established method of tracking. The point-to-point or path trajectory takes into consideration the actuator's large stroke span. Besides, the aim of this trajectory is to demonstrate the proposed control strategies' performance and capabilities in attaining high tracking performance for different set points throughout the actuator stroke. A continuous point-to-point trajectory, as illustrated in Fig. 9, is developed to facilitate a practical reference trajectory for tracking control in the EHA system where the actuator may track the required path accordingly. Furthermore, this form of trajectory is used to validate the proposed control strategies' ability to keep the actuator in a certain position under a variety of operating situations. Several studies have employed the related point-to-point-based trajectory tracking for the EHA system to assess the control strategies' efficacy [51], [52].

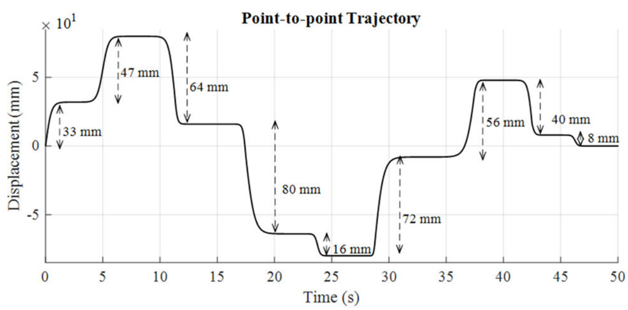

FIGURE 9. Point-to-point trajectory.

Meanwhile, a chaotic trajectory is designed by combining the characteristics of both a sinusoidal and a point-to-point trajectory [53], [54]. This trajectory can evaluate tracking performance for various set points during the actuator stroke. As a result, this trajectory is utilized in this research to evaluate the robustness of the EHA system with the proposed control strategies.

F. PERFORMANCE INDICATORS

The performance of the designed control strategies will be thoroughly studied and reported in time domains. Most tracking studies in the EHA system provide basic performance measures as an indication of the control strategies' capabilities, including absolute error (AE) [55], root mean square error (RMSE) [9], and mean square error (MSE) [7], [56], [57]. Consequently, the MSE and RMSE performance indicators written in (40) and (41), respectively were employed to provide performance metric that indicate the time-domain trajectory tracking capabilities.

$$MSE = \frac{\sum_{i=1}^{n} (r - x_p)^2}{n} \tag{40}$$

$$RMSE = \sqrt{\frac{\sum_{i=1}^{n} (r - x_p)^2}{n}} \tag{41}$$

The proposed control strategies' effectiveness and precision for the tracking control issue is defined by these performance indicators, which includes the tracking error written in (12) and the number of samples (n) obtained. In the next section, these performance indicators are utilized to analyze and discuss the performance of the EHA system with the proposed control strategies in comparison to the established control approaches, where a lower value of the RMSE indicator implies a better precision of trajectory tracking control in the EHA system with the designed control strategy.

In addition, the tracking control performance of the EHA system also requires investigations under various operating conditions to evaluate the robustness of the proposed control strategies. Therefore, a robustness test for the EHA system with the proposed control strategies was conducted in this research by reducing the supply pressure to reflect parameter fluctuations. The robustness measurement index (RI) is evaluated by determining the MSE obtained for the nominal (NOM) and variation (VAR) operating conditions which can be expressed as

$$RI\,(r, T) = \frac{|MSE\,(r, NOM, T) - MSE\,(r, VAR, T)|}{MSE\,(r, NOM, T)} \tag{42}$$

where r and T are reference trajectory and tracking process period, respectively. The nominal operating condition is referred to the EHA system's nominal operating supply pressure 8×10^6 Pa, and the variation operating condition is referred to 50% of the EHA system's nominal operating supply pressure [58]. The robustness index RI will be used to compare the tracking performance of the EHA system, where a lower value of the RI implies better robustness and demonstrates the capability of the proposed control strategies for the EHA system under uncertainty and disturbance conditions.

V. RESULTS AND DISCUSSIONS

This section presents and discusses the findings of simulations and real-time implementations of the SMC, FLSMC, SMCPID and FLSMCPID control strategies for the tracking control in the EHA system throughout four trajectories:

TABLE 1. Estimated parameters.

Parameter	Model	
	Nominal	Variation
a_0	7855	7805
a_1	372.3	370.9
a_2	144400	143000

TABLE 2. Optimized variables values using PSO algorithm.

Variable	Value			
	SMC	FLSMC	SMCPID	FLSMCPID
λ	299.9836	299.9859	-	-
ε	10.6086	9.5970	1.6175	2.9700
k	0.0830	0.2761	6.6351	10.4652
k_p	-	-	50.2076	50.1914
k_i	-	-	33.1126	33.5840
k_d	-	-	0.1932	0.2065

(1) sinusoidal, (2) multi-sinusoidal, (3) point-to-point, and (4) chaotic. In simulation, the designed SMC, FLSMC, SMCPID, and FLSMCPID control algorithms as in (17), (19), (23), and (24) were applied to the linear model of EHA system as described in (6) for the feedback configuration shown in Fig. 5. Meanwhile, the real-time implementations were performed using the EHA system workbench which is illustrated in Figs. 1 and 2 to verify and validate the trajectory tracking control performance of the designed control strategies. In addition, the linear nominal and variation models of the EHA system obtained from the grey-box identification approach and details on the robustness evaluations conducted based on the chaotic trajectory tracking under different operating supply pressures are included. Moreover, a discussion on the discrepancy between simulation and experimental works are also provided.

A. EHA SYSTEM: LINEAR MODEL

A linear mathematical model of an EHA system for both nominal and variation conditions were obtained using the grey-box identification approach. The nominal and variation conditions represent the operating supply pressure of 8 MPa and 4 MPa, respectively. It is estimated that the linear model of nominal and variation conditions can effectively represent the real EHA system dynamics at 89.01% and 89%, under the operating supply pressure of 8 MPa and 4 MPa, respectively, for 100 s of operation duration. The results are summarized in Table 1. It is revealed that decreasing nominal supply pressure by 50% decreased the value of the estimated parameters variation model relative to the nominal model. Therefore, the mathematical model structure based on the transfer function for nominal and variation conditions are expressed in (43) and (44), respectively.

$$\frac{X_p(s)}{U(s)} = \frac{144400}{s\left(s^2 + 372.3s + 7855\right)} \tag{43}$$

$$\frac{X_p(s)}{U(s)} = \frac{143000}{s\left(s^2 + 370.9s + 7805\right)} \tag{44}$$

B. PSO ALGORITHM: OPTIMUM VARIABLES VALUE

The PSO algorithm was used to determine the optimal variables value for the designed SMC, FLSMC, SMCPID, and FLSMCPID control algorithms. In summary, the values of the variables that reached the minimum fitness value upon the completion of the iteration procedure are considered the final optimum values of the designed control algorithms variables and are listed in Table 2. These variables values were subsequently enrolled into (17), (19), (23), and (24), respectively, for simulation and experimental implementation.

During the PSO implementation, the variables value was revised with each iteration to get the minimum fitness value. It is revealed that the FLSMC variables converge at 11th iteration, followed by the FLSMCPID variables at 15th iteration, the SMCPID variables at 17th iteration, and the SMC variables at 20th iteration. In addition, it is justifiable that the various convergence solutions emerged due to the action of the FL and signum functions.

C. SIMULATION AND EXPERIMENTAL RESULTS

The tracking responses of the EHA system are evaluated for 100 s for sinusoidal, multi-sinusoidal, point-to-point, and chaotic trajectories using 1 ms sample time. Trajectory tracking responses are observed and their related quantitative indicator values were collected. In addition to the simulations and experiments, the conventional SMC approach was assessed for performance comparisons with the FLSMC control strategy by implementing the control variables described in the previous section. Meanwhile, the performance of the SMCPID approach was compared to that of the FLSMCPID control strategy.

The simulated and experimental responses of the tracking performances for FLSMC are illustrated in Figs. 10, 11, 12, and 13. Comparing the FLSMC control strategy which utilizing a continuous fuzzy logic switching function to the SMC controller design which employing discontinuous signum switching function, the EHA system with the SMC approach produces a trajectory tracking performance that is inferior to that of the FLSMC control strategy. It is evident that using the SMC approach as opposed to the FLSMC control strategy resulted in a significant deviation from the reference trajectory during the tracking process due to the non-linearities such as backlash and friction in the EHA system. While the SMC approach showed significant effort in achieving the lowest tracking error, the FLSMC control strategy was able to maintain an acceptable performance.

Furthermore, Table 3 summarizes the quantitative indicator value of the MSE, RMSE, and RI achieved during all trajectories tracking in the EHA system with the designed control strategies and under the nominal and variation conditions for

TABLE 3. Summary of trajectory tracking performances.

Trajectory	Simulation - MSE (mm2)				Experiment - MSE (mm2)			
	SMC	FLSMC	SMCPID	FLSMCPID	SMC	FLSMC	SMCPID	FLSMCPID
Sinusoidal – 0.25 Hz	0.0792	0.0691	0.0048	0.0026	8.6913	2.3738	0.1380	0.0759
Multi-sinusoidal	3.1382	2.3793	0.0841	0.0482	3.1545	1.0783	0.0763	0.0479
Point-to-point	1.2450	0.6485	0.0642	0.0841	10.1512	6.3620	0.0266	0.0173
Chaotic (NOM)	2.7105	1.5180	0.3015	0.2118	20.5785	5.5345	0.1037	0.0694
Chaotic (VAR)	2.8361	1.5685	0.3193	0.2262	14.7318	5.5642	0.1372	0.0892
	Simulation - RMSE (mm)				Experiment - RMSE (mm)			
Sinusoidal – 0.25 Hz	0.2814	0.2629	0.0693	0.0510	2.9481	1.5407	0.3715	0.2755
Multi-sinusoidal	1.7715	1.5425	0.2900	0.2195	1.7761	1.0384	0.2762	0.2189
Point-to-point	1.1158	0.8053	0.2534	0.2900	3.1861	2.5223	0.1631	0.1315
Chaotic (NOM)	1.6464	1.2321	0.5491	0.4602	4.5364	2.3526	0.3220	0.2634
Chaotic (VAR)	1.6841	1.2524	0.5651	0.4756	3.8382	2.3589	0.3704	0.2987
	Simulation - RI				Experiment - RI			
	0.0463	0.0186	0.0066	0.0053	0.2841	0.0014	0.0016	0.0010

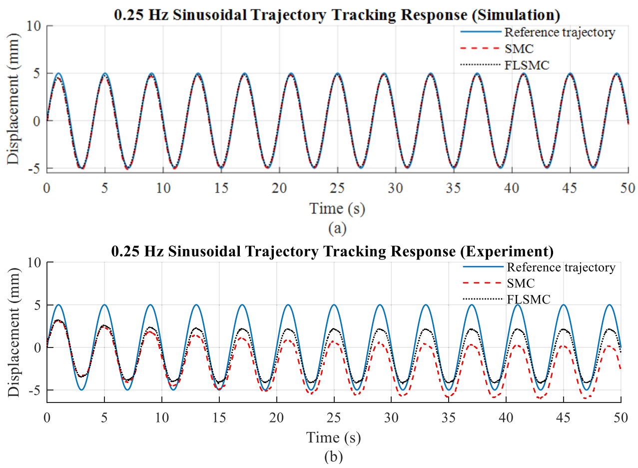

FIGURE 10. FLSMC: Tracking performance for sinusoidal trajectory.

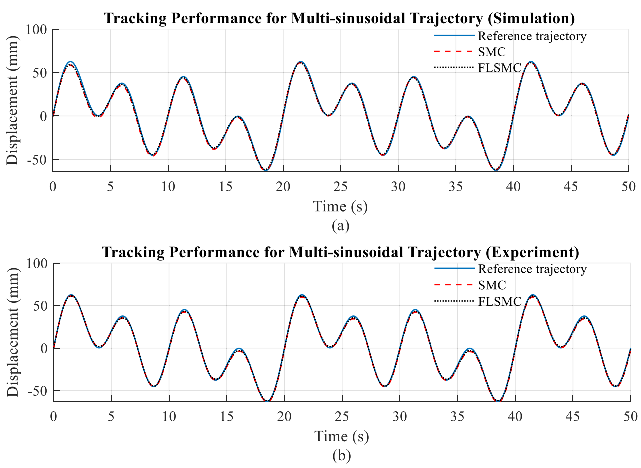

FIGURE 11. FLSMC: Tracking performance for multi-sinusoidal trajectory.

chaotic profile. It reveals that the proposed FLSMC control strategy is more capable of coping with reducing 50% of the supply pressure in the EHA system for 100 s of the real-time trajectory tracking implementation as compared to

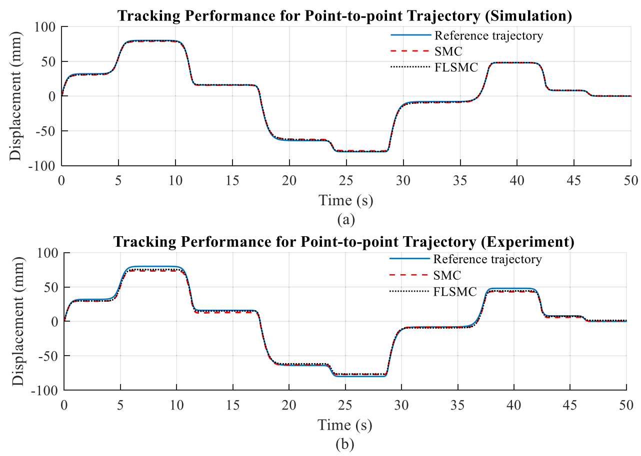

FIGURE 12. FLSMC: Tracking performance for point-to-point trajectory.

the SMC approach. Overall, comparing the simulation and experimental outcomes shows a similar pattern of results that verified the performance of the EHA system with the proposed FLSMC control strategy in term of tracking control effectiveness and precision evaluation. The results demonstrated that the proposed FLSMC control strategy confirmed superior effectiveness and precision as compared to the SMC approach during all trajectories tracking in the EHA system for both simulated and real-time implementations under the variation condition. Furthermore, the robustness test is performed with the purpose of analyzing the effect of plant parameter changes on the EHA system tracking performance with the designed control strategies. Comparison of the RI index for the simulated and real-time tracking performance shows that the EHA system with the FLSMC control strategy is more robust as compared to the SMC approach towards any changes in plant parameters and capable of maintaining the performance even though the control strategy is designed for a nominal point or certain operating range of actuator stroke. Therefore, significant effectiveness, precision, and robustness performance improvement of trajectory tracking

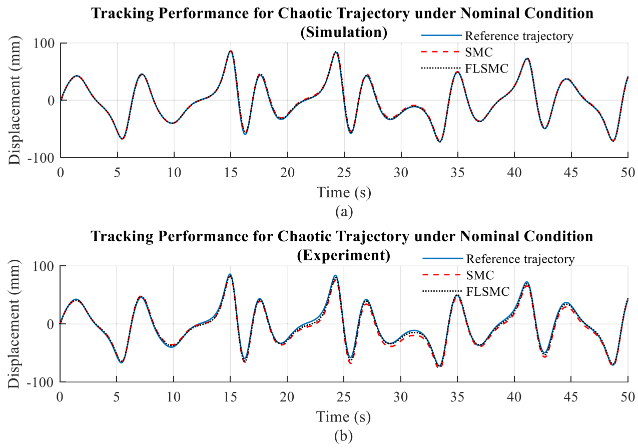

FIGURE 13. **FLSMC: Tracking performance for chaotic trajectory.**

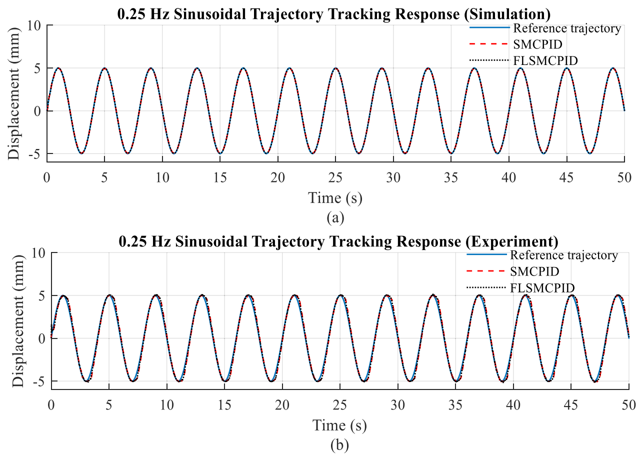

FIGURE 14. **FLSMCPID: Tracking performance for sinusoidal trajectory.**

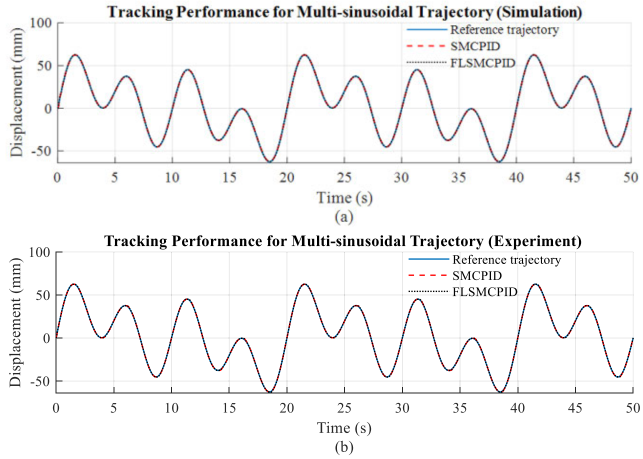

FIGURE 15. **FLSMCPID: Tracking performance for multi-sinusoidal trajectory.**

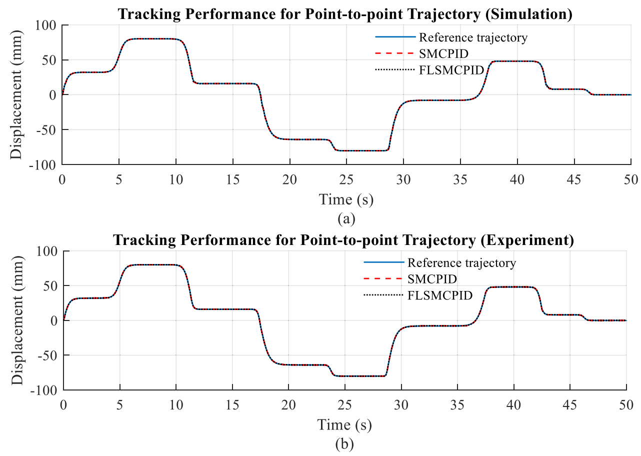

FIGURE 16. **FLSMCPID: Tracking performance for point-to-point trajectory.**

control in the EHA system can be seen by utilizing the continuous FL-based function to replace the signum function in the conventional SMC algorithm. The highest performance percentage of tracking control improvement is produced during the chaotic trajectory and is followed by the 0.25 Hz sinusoidal, multi-sinusoidal, and point-to-point trajectories. Observably, the point-to-point trajectory design feature consisting of different set points over 200 mm actuator stroke is the main cause that makes it difficult for the designed control strategies to produce higher performance. It is also revealed that the EHA system with the FLSMC control strategy is more robust compared to the SMC approach towards any changes in plant parameters and capable to maintain the performance even though the control strategy is designed for a nominal point or certain operating range of actuator stroke.

Meanwhile, Figs. 14, 15, 16, and 17 illustrate the simulated and experimental responses of the tracking performances for FLSMCPID. Observably, the EHA system with the SMCPID approach yields a trajectory tracking performance that is inferior to that of the FLSMCPID control strategy. It is evident that using SMCPID approach as opposed to the FLSMCPID control strategy resulted in a significant deviation from the reference trajectory. While the EHA system with the SMCPID approach shown significant effort in obtaining the lowest tracking error, the FLSMCPID control strategy was able to maintain a considerable performance.

Furthermore, based on Table 3, it is revealed that the EHA system with the FLSMCPID control strategy provides a significant improvement in tracking control effectiveness, precision, and robustness performances as compared to the SMCPID approach during the executions. Overall, the experimental findings reveal a similar pattern of improvement that validates the performance of the EHA system with the FLSMCPID control strategy in terms of tracking control effectiveness, precision, and robustness. Therefore, significant effectiveness, precision, and robustness performances improvement of trajectory tracking control in the EHA system can be seen by utilizing the hybrid PID control. In addition, a comparative performance of real-time tracking control between the FLSMC and FLSMCPID control strategies is details in Table 4. Moreover, Table 5 lists

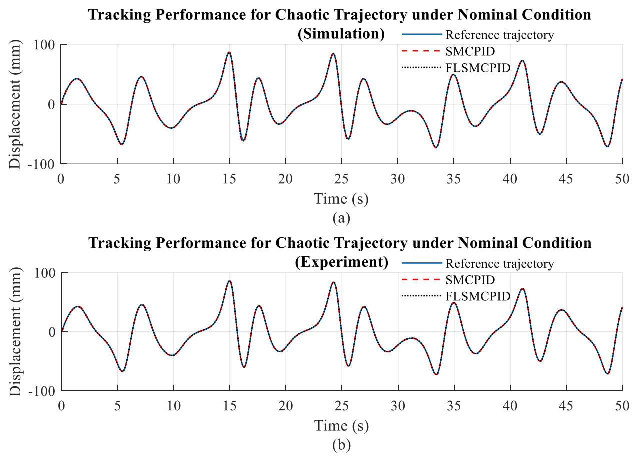

FIGURE 17. FLSMCPID: Tracking performance for chaotic trajectory.

the advantages and disadvantages of FLSMCPID control strategy.

In summary a comparative performance analysis is necessary to demonstrate the tracking control improvement between the FLSMC and FLSMCPID control where a significant improvement of effectiveness, precision, and robustness performances for the real-time trajectory tracking control in the EHA system is provided by utilizing the hybrid sliding surface with PID control in the FLSMC algorithm. It is revealed that the FLSMCPID control strategy is more effective and outperformed the FLSMC approach as it provided the lowest MSE indicator value during all trajectories tracking. The integration of PID with fuzzy sliding mode control optimizes control performance by boosting steady-state accuracy and transient response. The integral component of PID eradicates steady-state error, and the proportional and derivative components enhance transient response by minimizing overshoot and augmenting damping. This enhances the resilience and adaptability of fuzzy-SMC, yielding a more accurate, stable, and responsive control system despite nonlinearities and disturbances. The FLSMCPID control strategy is capable to provide a significant of 96.8%, 95.6%, 99.7%, and 98.8% effectiveness improvement for the 0.25 Hz sinusoidal, multi-sinusoidal, point-to-point, and chaotic trajectories tracking, respectively, as compared to the FLSMC approach. In addition, the results also indicated that the proposed FLSMCPID control strategy offered a better tracking precision as compared to the FLSMC approach. The FLSMCPID control strategy provided a precise improvement of 82.1%, 78.9%, 94.8%, and 88.8% for the 0.25 Hz sinusoidal, multi-sinusoidal, point-to-point, and chaotic trajectories tracking, respectively, as compared to the FLSMC approach. Furthermore, the robustness test is performed with the purpose of analyzing the effect of plant parameter changes on the EHA system tracking performance with the designed control strategies. Analysis of the RI index performance reveals that the FLSMCPID control strategy is more robust as compared to the FLSMC approach towards any changes in plant parameters and capable of maintaining the performance even though the control strategy is designed for a nominal point or certain operating range of actuator stroke. Compared to the FLSMC approach, the FLSMCPID control strategy improved the robustness performance by 33.3%. Therefore, this robust control strategy can be used to any actuator state that is known to be sensitive to non-linear uncertainties and disturbances. Overall, the analysis of the data obtained from the experimental implementations for the 0.25 Hz sinusoidal, multi-sinusoidal, point-to-point, and chaotic trajectory tracking control reveals a consistent pattern of findings that supports the improvement for the effectiveness, precision, and robustness performances of the proposed FLSMCPID control strategy as compared to the FLSMC approach.

D. DISCREPANCY BETWEEN SIMULATION AND EXPERIMENTAL IMPLEMENTATIONS

It is widely acknowledged that testing and implementation of SMC, FLSMC, SMCPID, and FLSMCPID controller designs could not realistically predict perfect one-to-one agreement or compliance between simulation and experimental execution due to various environmental factors such as modeling inaccuracies and operating conditions.

The real-time implementation of the designed controllers using a real EHA system should resemble the execution in the simulation study using the EHA system model. Through the literature study, it is known that the EHA system is a nonlinear system. However, a linear model for the EHA system obtained through grey-box identification is used during the simulation study. Moreover, the obtained linear model can only approximate the dynamics of the real EHA system to an extent of about 89%. As a result, it can be claimed that linearization in the EHA system model is one of the factors influencing performance discrepancy between simulations and experimental studies.

Furthermore, to carry out the real-time implementation of the designed controllers for various trajectory tracking, this research must compromise with the utilization of already-existing physical facilities and the available tools for designing and developing the EHA system workbench. In addition, in real-time implementation using the EHA system workbench, there are several disturbances that interrupt the assessment of tracking control performance, such as noise in the sensor, cylinder friction, and fluctuations in pressurized fluid temperature. However, the disturbances are being neglected in simulation studies. Therefore, it can be claimed that the disturbances neglection in simulation studies are also one of the factors influencing performance discrepancy between simulations and experimental studies.

Although there were small differences that were noted in the time-response, the simulation process provided characteristic behavior closely with the experimental platform in terms of quantitative measurements in which MSE, RMSE, and RI were used. In addition, similar trends in the evaluation process are obtained for both the implemented environments

TABLE 4. Summary of comparative real-time performance between the FLSMC and FLSMCPID.

Trajectory	MSE (mm2)		Improvement (%)	RMSE (mm)		Improvement (%)	RI		Improvement (%)
	FLSMC	FLSMCPID		FLSMC	FLSMCPID		FLSMC	FLSMCPID	
Sinusoidal – 0.25 Hz	2.3738	0.0759	96.8026	1.5407	0.2755	82.1185			
Multi-sinusoidal	1.0783	0.0479	95.5578	1.0384	0.2189	78.9195			
Point-to-point	6.3620	0.0173	99.7281	2.5223	0.1315	94.7865			
Chaotic (NOM)	5.5345	0.0694	98.7460	2.3526	0.2634	88.8039	0.0054	0.0036	33.3333
Chaotic (VAR)	5.5642	0.0892	98.3969	2.3589	0.2987	87.3373			

TABLE 5. Advantages and disadvantages of the proposed FLSMCPID.

No.	Advantages	Disadvantages
1	Improves performance by combining PID precision and SMC robustness.	Fuzzy inference delays control, especially in high-speed applications.
2	Improved steady-state accuracy through PID integral action	Fuzzy logic, PID, and SMC increase computing overhead.
3	Enhanced transient response with a reduced settling time	Complexity in multiple parameter tuning (PID gains, fuzzy rules, SMC values)
4	Increased adaptability through fuzzy logic in handling nonlinearities	The development of real-time systems may necessitate high-performance hardware, hence constraining low-cost applications.

and indicate that validation performed to meet the 'proof-of-concept' approach is acceptable.

VI. CONCLUSION AND FUTURE WORKS

An effective and precise trajectory tracking control with significant robustness is essential in industrial environments for the efficient operation of the EHA system. Due to its high robustness to uncertainties and disturbances, the trajectory tracking control employing the SMC approach has been identified as a very prospective solution for the EHA control systems. However, in actual deployments of the conventional SMC approach in the EHA system, high frequency-controlled valve activity has occurred, which has significantly affected the trajectory tracking control's performance. In these circumstances, it is difficult for the EHA system to accurately track the assigned trajectory with fast response operations. To address these challenges, this paper proposes FLSMCPID approach for effective and precise tracking control of a double-acting single-ended EHA system under varied trajectories and supply pressure variations. Apart from providing satisfying results of the trajectory tracking, the results revealed that the FLSMCPID control strategy provided higher robustness as compared to the SMCPID, FLSMC, and SMC approaches towards any changes in plant parameters and could maintain the performance even though the proposed control strategy is designed for a nominal point or certain operating range of actuator stroke. This approach's novel contribution is the synergistic employment of PID tuning for fine error correction, fuzzy logic for adaptive gain adjustment, and SMC for robustness, resulting in a controller that is both theoretically sound and practically practicable. This makes the FLSMCPID controller particularly interesting for real-world applications such as robotic systems, self-driving automobiles, and complex industrial processes that require both precision and durability.

There is a substantial potential that this research could be expanded to fulfill the desired industrial applications. The following recommendations are potential future research projects that would be advantageous for other researchers pursuing this area of study.

- The development of a complete model that closely resembles the real EHA system will offer the foundation for a thorough investigation of the system's dynamics. Thus, the design of a robust control strategy on such a model ensures the system can respond well under real physical conditions and is more directly applicable to real systems.
- Due to the limitations of the EHA system workbench, the robustness test is limited to supply pressure variations, whereas the effects of payload are also insignificant in the experimental study. Thus, it is desirable in the future to study the robustness of the proposed control strategy under a broader range of uncertainties and disturbances.
- In this study, the switching function in the proposed FLSMC control algorithm is designed based on the continuous FL function with a single-input and single-output structure, where three triangular input and output membership functions are used. Therefore, it is recommended that future research study the effect of expanding the input and output membership functions on the EHA system's performance.
- A comparison evaluation with related hybrid control systems would enhance the positioning of the FLSMCPID strategy within the broader area in future work. This may involve comparisons with methodologies such neuro-fuzzy controllers and adaptive SMC. Such

comparisons would provide a deeper comprehension of the relative advantages and disadvantages of any methodology. Moreover, enhancing the repeatability and applicability of outcomes in practical control applications necessitates the incorporation of specified test scenarios or benchmark systems.

- In order to bridge the gap between simulation and operational deployment, future research should also concentrate on validating the FLSMCPID controller through real-world applications. The controller's computational feasibility, adaptability, and robustness would be evaluated under actual operating conditions, including sensor noise, actuator limitations, and system uncertainties, by applying it to systems such as robotic manipulators, autonomous vehicles, or industrial process control. Additionally, the controller's efficacy would be demonstrated through real-world implementation, which would also assist in the identification of application-specific challenges and the development of additional refinements in design and tuning strategies.
- Although PID with FLSMC improves precision and robustness, some practical limitations must be addressed in future research. Fuzzy inference control delay can affect real-time performance in rapid or high-frequency systems. The computational expense of real-time fuzzy logic, sliding mode control, and PID may need high-performance hardware, limiting their use in low-cost or embedded devices. Scalability to multi-axis or higher-order systems is difficult because rule bases and control settings grow exponentially, causing instability or performance degradation. Future research should optimize fuzzy inference efficiency, reduce computing load using reduced rule sets or adaptive algorithms, and design scalable structures for complicated multi-input systems.

REFERENCES

[1] E. M. Herbert, *Hydraulic Control Systems*. New York, NY, USA: Wiley, 1967.

[2] M. Jelali and A. Kroll, *Hydraulic Servo-Systems: Modelling, Identification and Control*. Cham, Switzerland: Springer, 2003.

[3] R. Agarwala, "Development of a robust nonlinear pitch angle controller for a redesigned 5MW wind turbine blade tip," *Energy Rep.*, vol. 5, pp. 136–144, Nov. 2019, doi: 10.1016/j.egyr.2018.12.005.

[4] S. Chen, "Trajectory tracking and control algorithm for precision parallel robot," *J. Adv. Comput. Intell. Intell. Informat.*, vol. 23, no. 2, pp. 237–241, Mar. 2019, doi: 10.20965/jaciii.2019.p0237.

[5] S. Ge, R. Zhao, W. Li, J. Li, Y. Liu, and Z. Wang, "Sliding-mode control for coal shearer drum height adjustment based on variable speed reaching law," *J. Vibroengineering*, vol. 22, no. 8, pp. 1782–1797, Dec. 2020, doi: 10.21595/jve.2020.21223.

[6] B. Guo and J. Guo, "Feedback linearization and reaching law based sliding mode control design for nonlinear hydraulic turbine governing system," *Energies*, vol. 12, no. 12, p. 2273, Jun. 2019, doi: 10.3390/en12122273.

[7] J. Huang, H. An, Y. Yang, C. Wu, Q. Wei, and H. Ma, "Model predictive trajectory tracking control of electro-hydraulic actuator in legged robot with multi-scale online estimator," *IEEE Access*, vol. 8, pp. 95918–95933, 2020, doi: 10.1109/ACCESS.2020.2995701.

[8] X. Kong, H. Majumdar, F. Zang, S. Jiang, Q. Wu, and W. Zhang, "A multi-switching mode intelligent hybrid control of electro-hydraulic proportional systems," *Proc. Inst. Mech. Eng., C, J. Mech. Eng. Sci.*, vol. 233, no. 1, pp. 120–131, Jan. 2019, doi: 10.1177/0954406218756446.

[9] L. Cheng, Z.-C. Zhu, G. Shen, S. Wang, X. Li, and Y. Tang, "Real-time force tracking control of an electro-hydraulic system using a novel robust adaptive sliding mode controller," *IEEE Access*, vol. 8, pp. 13315–13328, 2020, doi: 10.1109/ACCESS.2019.2895595.

[10] D. Won, W. Kim, and M. Tomizuka, "Nonlinear control with high-gain extended state observer for position tracking of electro-hydraulic systems," *IEEE/ASME Trans. Mechatronics*, vol. 25, no. 6, pp. 2610–2621, Dec. 2020, doi: 10.1109/TMECH.2020.2985619.

[11] M. Yang, K. Ma, Y. Shi, and X. Wang, "Modeling and position tracking control of a novel circular hydraulic actuator with uncertain parameters," *IEEE Access*, vol. 7, pp. 181022–181031, 2019, doi: 10.1109/ACCESS.2019.2959296.

[12] L. Li, H. Huang, F. Zhao, J. W. Sutherland, and Z. Liu, "An energy-saving method by balancing the load of operations for hydraulic press," *IEEE/ASME Trans. Mechatronics*, vol. 22, no. 6, pp. 2673–2683, Dec. 2017, doi: 10.1109/TMECH.2017.2759228.

[13] J. Guo, S. Ma, X. Zhang, and X. Han, "Research on CNC machining technology of the upper shell of electro-hydraulic servo valve," *J. Phys., Conf. Ser.*, vol. 1635, no. 1, Nov. 2020, Art. no. 012016, doi: 10.1088/1742-6596/1635/1/012016.

[14] H. Liu, X. Zhang, L. Quan, and H. Zhang, "Research on energy consumption of injection molding machine driven by five different types of electro-hydraulic power units," *J. Cleaner Prod.*, vol. 242, Jan. 2020, Art. no. 118355, doi: 10.1016/j.jclepro.2019.118355.

[15] S. Zhang, T. Minav, M. Pietola, H. Kauranne, and J. Kajaste, "The effects of control methods on energy efficiency and position tracking of an electro-hydraulic excavator equipped with zonal hydraulics," *Autom. Construct.*, vol. 100, pp. 129–144, Apr. 2019, doi: 10.1016/j.autcon.2019.01.003.

[16] W. Wang, B. Zhang, Y. Li, W. Dou, X. Yang, J. Liu, and X. Wang, "Research on large-diameter electro-hydraulic rotary table and its control system for deep-water drilling rig," *J. Phys., Conf. Ser.*, vol. 1601, no. 2, Jul. 2020, Art. no. 022030, doi: 10.1088/1742-6596/1601/2/022030.

[17] B. Xu, J. Shen, S. Liu, Q. Su, and J. Zhang, "Research and development of electro-hydraulic control valves oriented to Industry 4.0: A review," *Chin. J. Mech. Eng.*, vol. 33, no. 1, pp. 1–20, Dec. 2020, doi: 10.1186/s10033-020-00446-2.

[18] Q. Zhang, X. Kong, B. Yu, K. Ba, Z. Jin, and Y. Kang, "Review and development trend of digital hydraulic technology," *Appl. Sci.*, vol. 10, no. 2, p. 579, Jan. 2020, doi: 10.3390/app10020579.

[19] F. Bechet, K. Ogawa, E. Sariyildiz, and K. Ohnishi, "Electrohydraulic transmission system for minimally invasive robotics," *IEEE Trans. Ind. Electron.*, vol. 62, no. 12, pp. 7643–7654, Dec. 2015, doi: 10.1109/TIE.2015.2453930.

[20] T. Park, K. Kim, S.-R. Oh, and Y. Cha, "Electrohydraulic actuator for a soft gripper," *Soft Robot.*, vol. 7, no. 1, pp. 68–75, Feb. 2020, doi: 10.1089/soro.2019.0009.

[21] X. Chen, Z. Jiao, X. Liu, X. Li, P. Qi, and Y. Shang, "Experimental validation of a practical nonlinear control method for hydraulic flight motion simulator," *J. Franklin Inst.*, vol. 359, no. 6, pp. 2405–2423, Apr. 2022, doi: 10.1016/j.jfranklin.2022.02.013.

[22] W. Deng, J. Yao, Z. Jiao, and X. Liu, "High dynamic output feedback robust control of hydraulic flight motion simulator using a novel cascaded extended state observer," *Chin. J. Aeronaut.*, vol. 35, no. 7, pp. 300–309, Jul. 2022, doi: 10.1016/j.cja.2021.07.013.

[23] Z. Jiao, X. Chen, X. Liu, X. Li, P. Qi, Y. Shang, and W. Qiao, "An experimental study on outer frame position control of hydraulic flight motion simulator with model compensation," *IEEE/ASME Trans. Mechatronics*, vol. 27, no. 5, pp. 3419–3428, Oct. 2022, doi: 10.1109/TMECH.2021.3140079.

[24] H. Songshan, J. Zongxia, W. Chengwen, and S. Yaoxing, "Fuzzy robust nonlinear control approach for electro-hydraulic flight motion simulator," *Chin. J. Aeronaut.*, vol. 28, no. 1, pp. 294–304, Feb. 2015, doi: 10.1016/j.cja.2014.12.025.

[25] Y. Ren, J. Bai, and J. Ruan, "Design, modeling and experimental validation of a variable resonant electro-hydraulic fatigue testing system," *IEEE Access*, vol. 7, pp. 180835–180845, 2019, doi: 10.1109/ACCESS.2019.2957126.

[26] V. V. Klimov, "Geomechanical feasibility of underground coal mining technology using control systems of electro-hydraulic shield supports for longwall mining," *IOP Conf. Ser., Mater. Sci. Eng.*, vol. 560, no. 1, Jun. 2019, Art. no. 012067, doi: 10.1088/1757-899x/560/1/012067.

[27] D. Szurgacz, "Electrohydraulic control systems for powered roof supports in hazardous conditions of mining tremors," *J. Sustain. Mining*, vol. 14, no. 4, pp. 157–163, 2015, doi: 10.1016/j.jsm.2015.12.001.

[28] J. Liu and X. Wang, *Advanced Sliding Mode Control for Mechanical Systems*. Berlin, Germany: Springer, 2012.

[29] V. Utkin, "Variable structure systems with sliding modes," *IEEE Trans. Autom. Control*, vol. AC-22, no. 2, pp. 212–222, Apr. 1977.

[30] V. Utkin and H. Lee, "Chattering problem in sliding mode control systems," *IFAC Proc. Volumes*, vol. 39, no. 5, 2006, doi: 10.3182/20060607-3-it-3902.00003.

[31] A. T. Thomas, R. Parameshwaran, S. Sathiyavathi, and A. V. Starbino, "Improved position tracking performance of electro hydraulic actuator using PID and sliding mode controller," *IETE J. Res.*, vol. 68, no. 3, pp. 1683–1695, Oct. 2019, doi: 10.1080/03772063.2019.1664341.

[32] M. Yang, Q. Zhang, X. Lu, R. Xi, and X. Wang, "Adaptive sliding mode control of a nonlinear electro-hydraulic servo system for position tracking," *Mechanics*, vol. 25, no. 4, pp. 283–290, Aug. 2019, doi: 10.5755/j01.mech.25.4.22822.

[33] Z. Chen, X. Yuan, Y. Yuan, X. Lei, and B. Zhang, "Parameter estimation of fuzzy sliding mode controller for hydraulic turbine regulating system based on HICA algorithm," *Renew. Energy*, vol. 133, pp. 551–565, Apr. 2019, doi: 10.1016/j.renene.2018.10.061.

[34] S. Han, "Grey wolf and weighted whale algorithm optimized IT2 fuzzy sliding mode backstepping control with fractional-order command filter for a nonlinear dynamic system," *Appl. Sci.*, vol. 11, no. 2, p. 489, Jan. 2021, doi: 10.3390/app11020489.

[35] H. H. Tang and N. S. Ahmad, "Fuzzy logic approach for controlling uncertain and nonlinear systems: A comprehensive review of applications and advances," *Syst. Sci. Control Eng.*, vol. 12, no. 1, Dec. 2024, doi: 10.1080/21642583.2024.2394429.

[36] N. H. M. Ali, R. Ghazali, A. W. Tahir, H. I. Jaafar, M. F. Ghani, C. C. Soon, and Z. Has, "Enhanced hybrid robust fuzzy-PID controller for precise trajectory tracking electro-hydraulic actuator system," *Int. J. Robot. Control Syst.*, vol. 4, no. 2, pp. 795–813, May 2024, doi: 10.31763/ijrcs.v4i2.1407.

[37] B. H. G. Barbosa, L. A. Aguirre, C. B. Martinez, and A. P. Braga, "Black and gray-box identification of a hydraulic pumping system," *IEEE Trans. Control Syst. Technol.*, vol. 19, no. 2, pp. 398–406, Mar. 2011, doi: 10.1109/TCST.2010.2042600.

[38] A. Gmerek, N. Meskin, and F. Jaber, "Development of LPV models and switching LPV-H_∞ controller for a hydraulic system," in *Proc. Int. Conf. Control, Decis. Inf. Technol. (CoDIT)*, Apr. 2016, pp. 484–489, doi: 10.1109/CODIT.2016.7593610.

[39] J. Mozaryn, A. Winnicki, and M. Micewicz, "Experimental verification of discrete linear-quadratic-Gaussian control system of electro-hydraulic servodrive," in *Proc. 23rd Int. Conf. Methods Models Autom. Robot. (MMAR)*, Aug. 2018, pp. 241–246, doi: 10.1109/MMAR.2018.8486081.

[40] S. Vásquez, M. Kinnaert, and R. Pintelon, "Active fault diagnosis on a hydraulic pitch system based on frequency-domain identification," *IEEE Trans. Control Syst. Technol.*, vol. 27, no. 2, pp. 663–678, Mar. 2019, doi: 10.1109/TCST.2017.2772890.

[41] X. W. Liang, A. 'A. M. Faudzi, and Z. H. Ismail, "System identification and model predictive control using CVXGEN for electro-hydraulic actuator," *Int. J. Integr. Eng.*, vol. 11, no. 4, pp. 166–174, Sep. 2019, doi: 10.30880/ijie.2019.11.04.018.

[42] N. H. M. Ali, R. Ghazali, N. Rahzani, H. I. Jaafar, M. F. Ghani, and C. C. Soon, "Analyzing model order estimation in industrial hydraulics system using open loop identification," in *Proc. IEEE 14th Int. Conf. Control Syst., Comput. Eng. (ICCSCE)*, Aug. 2024, pp. 144–149, doi: 10.1109/ICCSCE61582.2024.10696387.

[43] N. H. M. Ali, R. Ghazali, H. I. Jaafar, M. F. Ghani, C. C. Soon, and Z. Has, "Comparison study between open-loop and closed-loop identification for industrial hydraulics actuator system," *Int. J. Mech. Eng. Robot. Res.*, vol. 13, no. 5, pp. 516–521, 2024, doi: 10.18178/ijmerr.13.5.516-521.

[44] R. Ghazali, C. C. Soon, H. I. Jaafar, Y. M. Sam, and M. F. Rahmat, "System identification of electro-hydraulic actuator system with pressure and load effects," in *Proc. IEEE Int. Conf. Control Syst., Comput. Eng. (ICCSCE)*, Nov. 2014, pp. 256–260, doi: 10.1109/ICCSCE.2014.7072726.

[45] S. Salleh, M. F. Rahmat, S. M. Othman, and K. A. Danapalasingam, "Review on modeling and controller design of hydraulic actuator systems," *Int. J. Smart Sens. Intell. Syst.*, vol. 8, no. 1, pp. 338–367, Jan. 2015, doi: 10.21307/ijssis-2017-762.

[46] T. Knohl and H. Unbehauen, "Adaptive position control of electrohydraulic servo systems using ANN," *Mechatronics*, vol. 10, nos. 1–2, pp. 127–143, Feb. 2000, doi: 10.1016/s0957-4158(99)00054-9.

[47] Zulfatman and M. F. Rahmat, "Application of self-tuning fuzzy PID controller on industrial hydraulic actuator using system identification approach," *Int. J. Smart Sens. Intell. Syst.*, vol. 2, no. 2, pp. 246–261, 2009.

[48] J. Kumar, A. T. Azar, V. Kumar, and K. P. S. Rana, "Design of fractional order fuzzy sliding mode controller for nonlinear complex systems," in *Mathematical Techniques of Fractional Order Systems*. Amsterdam, The Netherlands: Elsevier, 2018, pp. 249–282, doi: 10.1016/B978-0-12-813592-1.00009-X.

[49] C. M. Shern, R. Ghazali, C. S. Horng, H. I. Jaafar, C. C. Soon, and Y. M. Sam, "Performance analysis of position tracking control with PID controller using an improved optimization technique," *Int. J. Mech. Eng. Robot. Res.*, vol. 8, no. 3, pp. 401–405, 2019, doi: 10.18178/ijmerr.8.3.401-405.

[50] H. Du, L. Wang, J. Chen, H. Huang, and X. Feng, "Integral sliding-mode tracking control for heavy vehicle electrohydraulic power steering system," *IEEE/ASME Trans. Mechatronics*, vol. 26, no. 3, pp. 1455–1466, Jun. 2021, doi: 10.1109/TMECH.2020.3020956.

[51] M. E. M. Essa, M. A. S. Aboelela, M. A. M. Hassan, and S. M. Abdrabbo, "Hardware in the loop of position tracking control of hydraulic servo mechanism," in *Proc. 13th Int. Comput. Eng. Conf. (ICENCO)*, Dec. 2017, pp. 160–165, doi: 10.1109/ICENCO.2017.8289781.

[52] X. Jiang and C. Gosselin, "Dynamic point-to-point trajectory planning of a three-DOF cable-suspended parallel robot," *IEEE Trans. Robot.*, vol. 32, no. 6, pp. 1550–1557, Dec. 2016, doi: 10.1109/TRO.2016.2597315.

[53] G. Chen and T. Ueta, "Yet another chaotic attractor," *Int. J. Bifurcation Chaos*, vol. 9, no. 7, pp. 1465–1466, Jul. 1999, doi: 10.1142/s0218127499001024.

[54] A. G. Loukianov, J. Rivera, Y. V. Orlov, and E. Y. M. Teraoka, "Robust trajectory tracking for an electrohydraulic actuator," *IEEE Trans. Ind. Electron.*, vol. 56, no. 9, pp. 3523–3531, Sep. 2009, doi: 10.1109/TIE.2008.2010207.

[55] G. Palli, S. Strano, and M. Terzo, "A novel adaptive-gain technique for high-order sliding-mode observers with application to electro-hydraulic systems," *Mech. Syst. Signal Process.*, vol. 144, Oct. 2020, Art. no. 106875, doi: 10.1016/j.ymssp.2020.106875.

[56] N. Cisneros, A. J. Rojas, and H. Ramirez, "Port-Hamiltonian modeling and control of a micro-channel experimental plant," *IEEE Access*, vol. 8, pp. 176935–176946, 2020, doi: 10.1109/ACCESS.2020.3026653.

[57] X. Ji, Y. Ren, H. Tang, and J. Xiang, "DSmT-based three-layer method using multi-classifier to detect faults in hydraulic systems," *Mech. Syst. Signal Process.*, vol. 153, May 2021, Art. no. 107513, doi: 10.1016/j.ymssp.2020.107513.

[58] A. Bonchis, P. I. Corke, and D. C. Rye, "Experimental evaluation of position control methods for hydraulic systems," *IEEE Trans. Control Syst. Technol.*, vol. 10, no. 6, pp. 876–882, Nov. 2002, doi: 10.1109/TCST.2002.804128.

MUHAMAD FADLI GHANI (Member, IEEE) received the B.Eng. degree in electrical engineering (instrumentation and control) and the M.Eng. degree in electrical from Universiti Teknologi Malaysia, in 2008 and 2015, respectively, and the Ph.D. degree in electrical engineering from Universiti Teknikal Malaysia Melaka (UTeM), in 2023. He is currently a Senior Lecturer with the Faculty of Electrical Engineering, Universiti Teknologi Malaysia, and an Associate Research Fellow with the Centre for Artificial Intelligence and Robotics (CAIRO).

AHMAD ATHIF MOHD FAUDZI (Senior Member, IEEE) received the B.Eng. degree in computer engineering and the M.Eng. degree in mechatronics and automatic control from Universiti Teknologi Malaysia, Malaysia, in 2004 and 2006, respectively, and the Dr.Eng. degree in system integration from Okayama University, Japan, in 2010. He is currently a Research Fellow with the Centre for Artificial Intelligence and Robotics (CAIRO) and a Professor with the Faculty of Electrical Engineering, Universiti Teknologi Malaysia. He is mainly engaged in the research fields of soft actuators, inspection robotics, and bioinspired robotics.

ROZAIMI GHAZALI (Senior Member, IEEE) received the B.Eng. degree in electrical engineering (instrumentation and control) and the Ph.D. degree in electrical engineering from Universiti Teknologi Malaysia (UTM), in 2008 and 2013, respectively. He is currently an Associate Professor with Universiti Teknikal Malaysia Melaka (UTeM). His research interests include system identification and robust controller.

SHAHROL MOHAMADDAN received the B.Eng. and M.Eng. degrees in mechanical engineering from Shibaura Institute of Technology, Japan, in 2005 and 2007, respectively, and the Ph.D. degree from Loughborough University, U.K. He is currently an Associate Professor with the Innovative Global Program, College of Engineering, Shibaura Institute of Technology. His research interests include biomedical engineering and ergonomics.